Received: 2 April 2026 | Revised: 18 May 2026 | Accepted: 28 May 2026

DOI: 10.1002/alz.71611

Alzheimer's & Dementia®
THE JOURNAL OF THE ALZHEIMER'S ASSOCIATION

RESEARCH ARTICLE

Blood-based proteomic signature of amyloidosis: identification of novel regulators of amyloid load

Yike Chen[1,2] | Michael R. Duggan[3] | Jigyasha Timsina[1,2] | Ying Xu[1,2] | Daniel Western[1,2] | Katherine Gong[1,2] | Menghan Liu[1,2] | John Budde[1,2] | Suzanne E. Schindler[4] | John C. Morris[4] | David M. Holtzman[4] | Tammie L. S. Benzinger[5] | Brian A. Gordon[4] | Mahdi Moqri[6] | Knight Alzheimer Disease Research Center (Knight-ADRC)[7] | Laura Ibanez[1,2,4,8] | Keenan A. Walker[3] | Carlos Cruchaga[1,2,4,8,9] | Muhammad Ali[1,2]

[1]Department of Psychiatry, Washington University School of Medicine, St. Louis, Missouri, USA

[2]NeuroGenomics and Informatics Center, Washington University School of Medicine, St. Louis, Missouri, USA

[3]Laboratory of Behavioral Neuroscience, National Institute on Aging, Baltimore, Maryland, USA

[4]Department of Neurology, Washington University School of Medicine, St. Louis, Missouri, USA

[5]Department of Radiology, Washington University School of Medicine, St. Louis, Missouri, USA

[6]Division of Genetics, Department of Medicine, Brigham and Women's Hospital, Harvard Medical School, Boston, Massachusetts, USA

[7]Knight Alzheimer's Disease Research Center, Washington University, St. Louis, Missouri, USA

[8]Hope Center for Neurological Disorders, Washington University, St. Louis, Missouri, USA

[9]Department of Genetics, Washington University School of Medicine, St. Louis, Missouri, USA

Correspondence
Muhammad Ali, Washington University, School of Medicine, St. Louis, 63110, MO, USA.
Email: m.ali@wustl.edu

Funding information
Alzheimer's Association, Grant/Award Number: ZEN-22-848604; Foundation for the National Institutes of Health, Grant/Award Number: R01AG044546

Abstract

INTRODUCTION: Cerebral amyloidosis is a defining feature of Alzheimer's disease (AD), yet the molecular heterogeneity among amyloidbeta-positive (Aβ+) individuals remains poorly defined. We aimed to map the proteomic correlates of cerebral amyloidosis and link them to clinical variability within Aβ+ individuals.

METHODS: We integrated quantitative amyloid PET with large-scale plasma proteomics (~7000 proteins; SomaScan version 4.1) in Knight Alzheimer's Disease Research Center and Bio-Hermes cohorts (n = 1429). Proteome-wide association analyses identified proteins associated with amyloid load, followed by unsupervised clustering and pathway enrichment analyses.

RESULTS: We identified 454 amyloid-associated proteins, of which 54 replicated cross-cohort. A derived 54-protein proteomic score correlated with amyloid burden, AD biomarkers, and clinical severity. Pathway analyses of clinically distinct protein clusters revealed coordinated enrichment of intracellular signaling, immune, and proteostasis modules.

DISCUSSION: These findings delineate the circulating proteomic signature of cerebral amyloidosis and support plasma proteomics as a complementary approach to phosphorylated tau at threonine 217 and amyloid PET for biological stratification and characterization of disease heterogeneity in AD.

KEYWORDS
Alzheimer's disease, amyloidosis, dementia, plasma biomarkers, proteomics

Highlights

- Plasma proteomics identified reproducible amyloid-associated signatures across cohorts.
- 454 nominal proteins revealed widespread molecular variation in amyloid pathology.
- A 54-protein panel captured heterogeneity within Aβ+ individuals.
- Protein modules were associated with cognitive and biomarker variation.

1 | BACKGROUND

Alzheimer's disease (AD) is a progressive neurodegenerative disorder characterized by the accumulation of amyloid beta (Aβ) plaques and tau neurofibrillary tangles that lead to neuronal loss and cognitive decline.[1] While cerebrospinal fluid (CSF) and positron emission tomography (PET) biomarkers of Aβ and tau have transformed the diagnostic landscape of AD,[2] these modalities are limited by invasiveness, cost, and accessibility. Blood-based biomarkers are increasingly recognized as scalable and minimally invasive tools for the early detection and monitoring of AD pathology, with recent studies demonstrating strong a correspondence between plasma measures of phosphorylated tau isoforms (e.g., p-tau217 and p-tau181) and amyloid PET status.[2,3] However, despite major advances in candidate biomarker discovery, a deeper understanding of how peripheral protein changes relate to amyloid pathology and clinical progression remains incomplete.

Proteomic profiling offers a means to capture the complex molecular heterogeneity of AD across multiple biological compartments.[4–8] High-throughput platforms such as SomaScan and Olink enable simultaneous quantification of thousands of plasma proteins with high sensitivity, facilitating the discovery of molecular signatures linked to disease risk, progression, and resilience.[9,10] Recent large-scale studies have revealed peripheral proteomic patterns that reflect brain amyloidosis, neuroinflammation, and metabolic dysregulation, underscoring the potential of plasma proteomics as a readout of AD-related biology.[4–6,11] Integrative analyses combining plasma or CSF proteomics with amyloid PET have identified dozens to hundreds of proteins, including circulating immune mediators, lipoproteins, synaptic markers, and complement components, as correlates of amyloid pathology.[12–15] Nonetheless, the molecular specificity and heterogeneity among individuals with elevated amyloid burden remain incompletely characterized. Most prior work relied on dichotomous comparisons based on case-control or amyloid status, which may obscure continuous relationships between proteomic variation and amyloid load across the AD continuum. Moreover, the biological diversity among Aβ-positive (Aβ+) individuals, who range from asymptomatic to cognitively impaired, is poorly understood and motivates data-driven molecular stratification approaches that relate proteomic signatures to specific clinical trajectories.

In this study, we integrated quantitative amyloid PET with large-scale plasma proteomic profiling to identify circulating molecular correlates of cerebral amyloid burden. Proteome-wide analyses using both continuous and dichotomized PET measures first captured proteins associated with amyloidosis across its full spectrum, followed by focused analyses within Aβ+ individuals to identify proteins linked to higher amyloid load. Proteins showing reproducible associations across independent cohorts were then combined to derive a standardized 54-protein proteomic score (z) that summarized amyloid-associated molecular variation. We further examined these proteins and the composite score in relation to clinical and molecular AD endophenotypes, revealing coordinated protein clusters associated with traits such as earlier disease onset and greater cognitive impairment. Pathway enrichment analyses provided biological context, highlighting the convergence of synaptic, immune, metabolic, and proteostasis-related processes within the amyloid-associated proteomic signature. Together, this work outlines the circulating proteomic landscape of amyloidosis and introduces a reproducible plasma-based signature that complements established biomarkers such as Aβ and phosphorylated tau at threonine 217 (p-tau217), enabling finer molecular stratification of Aβ+ individuals while reducing reliance on invasive or costly CSF and imaging measures that are not readily suited for longitudinal disease monitoring.

RESEARCH IN CONTEXT

1. **Systematic review**: We searched PubMed for studies on plasma proteomics and cerebral amyloidosis in AD. Prior work has identified plasma biomarkers such as p-tau217 and several proteomic signatures associated with amyloid pathology. However, most studies rely on case-control or amyloid status (positive vs negative) comparisons and do not address molecular heterogeneity within Aβ+ individuals or reproducibility across cohorts.
2. **Interpretation**: We integrated amyloid PET with large-scale plasma proteomics across two independent cohorts to identify reproducible amyloid-associated proteins and derive a 54-protein signature of amyloid-related molecular variation. By focusing on Aβ+ individuals, we uncovered consistent associations with cognitive and biomarker measures and delineated distinct protein modules that define divergent clinical trajectories.
3. **Future directions**: Future work incorporating longitudinal plasma proteomics, multi-omics integration, and larger, harmonized cohorts will be important to characterize dynamic changes in amyloid-related protein networks and to evaluate their prognostic value.

2 | METHODS

2.1 | Study design and participant details

We designed a two-stage study to identify and validate plasma proteomic signatures associated with amyloid burden as measured by quantitative amyloid PET (Figure 1). The discovery cohort (Knight-ADRC) included 558 participants, of whom 178 were Aβ+ and 380 were amyloid-negative (Aβ–), based on PET-derived standardized uptake value ratios (SUVRs). All participants underwent plasma proteomic profiling using the SomaScan version 4.1 platform. A validation cohort of 871 individuals (241 Aβ+ and 630 Aβ–) with available amyloid PET and plasma proteomics was used to validate the findings (Table 1).

In the discovery stage, proteomic association with quantitative amyloid PET levels were assessed using linear regression models. The identified proteins were further tested for their associations with related clinical and biomarker traits, including Clinical Dementia Rating (CDR), Mini-Mental State Examination (MMSE), age at onset, CSF $A\beta_{42}$ (A), $A\beta_{40}$, and p-tau181 (T) biomarker status. An amyloid-associated proteomic score (z) was generated as the z-transformed weighted sum of standardized protein abundances, using effect size estimates from regression models of continuous amyloid PET levels among Aβ+ individuals as weights. Biological interpretation was performed by clustering proteins according to shared trait associations, followed by pathway enrichment analysis. A completely independent validation of protein correlation with quantitative Aβ+ levels and weighted proteomic score (z) association with clinical status and AD biomarkers was assessed in the external Bio-Hermes validation cohort.

TABLE 1 Demographic information of participants at time of plasma collection.

Characteristics	Knight-ADRC	Bio-Hermes
Sample size (N)	558	871
Mean age (SD)	68.5 (9.3)	71.9 (6.7)
Male (%)	45.9	42.7
APOE ε4+	229 (41.1%)	325 (37.3%)
Positive (Aβ+)	178 (32%)	241 (28%)
Tracer	PiB (n = 320), FBP (n = 238)	FBP (n = 871)

Note: Basic demographic information of plasma proteomics from discovery (Knight-ADRC) and validation (Bio-Hermes) cohorts. For each cohort we report the total sample size (*N*), mean age and its standard deviation (SD), percentage (%) of males, number of *APOE* ε4+ individuals and Aβ PET-positive (Aβ+) individuals, and tracer used to measure the amyloid PET burden.
Abbreviations: FBP, florbetapir F-18; Knight-ADRC, Knight Alzheimer Disease Research Center; PiB, ^{11}C-Pittsburgh compound-B; SD, standard deviation.

2.2 | Knight-ADRC

The Knight Alzheimer's Disease Research Center (Knight-ADRC) cohort at Washington University School of Medicine has been recruiting and longitudinally assessing community-dwelling adults older than 45 years old since 1979. The Memory and Aging Project (MAP) at the Knight-ADRC collects biofluids and conducts annual clinical assessments, neuropsychological testing, neuroimaging studies, and autopsies of brain samples. Eligible participants may be asymptomatic or have mild dementia at the time of enrollment. All participants are required to participate in core study procedures, including annual clinical assessments, neuropsychological testing, neuroimaging, and biofluid biomarker studies. Annual cognitive assessments of the participants were conducted by experienced clinicians. These assessments involved a semi-structured interview with both a knowledgeable collateral source and the individual displaying symptoms. The assessments followed the Uniform Data Set protocol of the National Alzheimer's Coordinating Center[16] and included a comprehensive neurological examination.

2.3 | Bio-Hermes

Between April 2021 and November 2022, 17 research sites collectively recruited 1296 community-based participants, of whom 1001 were enrolled in the Bio-Hermes Study.[17] These sites, all active in clinical trials evaluating investigational treatments for AD, have extensive expertise in recruiting individuals across the cognitive spectrum,

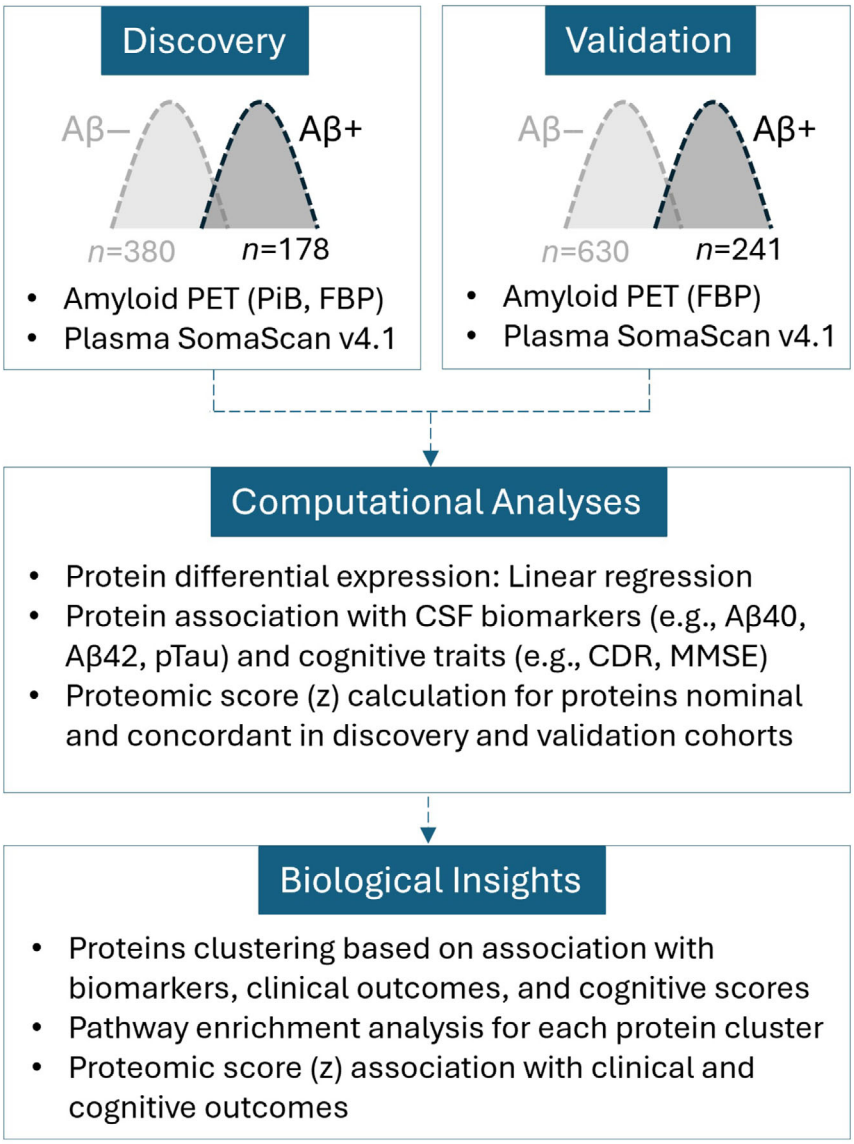

FIGURE 1 Study design and analytical workflow. Plasma proteomic signatures of amyloid load were investigated using a two-stage design. In the Knight-ADRC discovery cohort ($n = 558$; 178 Aβ+ and 380 Aβ−), participants underwent amyloid PET imaging using florbetapir F-18 (FBP) or ^{11}C-Pittsburgh compound-B (PiB) tracers and plasma proteomic profiling with the SomaScan version 4.1 platform. Findings were validated in an independent Bio-Hermes cohort ($n = 871$; 241 Aβ+ and 630 Aβ−) with amyloid PET (PiB) and the same proteomic platform. Computational analyses included (i) regression models testing associations between individual plasma proteins and continuous or dichotomized amyloid PET; (ii) association analyses of amyloid-related proteins with CSF biomarkers (e.g., Aβ42, Aβ40, Aβ42/Aβ40 ratio) and cognitive traits (e.g., CDR, MMSE); and (iii) calculation of a standardized proteomic score (z) based on 54 proteins that showed replicated associations with amyloid load across discovery and validation cohorts. Biological interpretation focused on clustering amyloid-associated proteins by their patterns of association with biomarkers and clinical outcomes, followed by pathway enrichment analyses for each protein cluster to highlight underlying molecular processes.

including cognitively normal controls (CO), those with mild cognitive impairment (MCI), and those with mild AD. Each site also has prior experience conducting studies requiring confirmed brain amyloid positivity as part of enrollment criteria. Plasma was collected using standardized protocols and frozen at −80°C until analysis. Cerebral Aβ was assessed with amyloid PET using the florbetapir F-18 (18F-AV-45) tracer and with plasma p-tau217 (Eli Lilly). Associations of SomaScan proteomic measurements with PET outcomes used blood samples collected at the most recent Bio-Hermes study visit at which PET data were collected.

2.4 | Plasma proteomics measurement and quality control

The proteomic data utilized in this study were obtained from in-house generated (Knight-ADRC)[18] and an external (Bio-Hermes) cohort (Table 1). For both cohorts, baseline plasma samples were analyzed using the SomaScan v4.1 platform, which measures more than 7,000 aptamers using an aptamer-based technology widely recognized for biomarker discovery.[19,20] This platform has demonstrated high reproducibility in prior studies, with median coefficients of variation for intra- and inter-plate assessments averaging around 5%.[21,22] It can detect proteins over a vast dynamic range, from femtomolar to micromolar concentrations, providing a sensitivity that exceeds that of traditional immunoassays.

For the Knight-ADRC plasma samples collection and proteomic data quality check and normalization was performed as described previously.[19,23] Briefly, plasma samples were collected in the morning without fasting. All samples followed standardized preparation and processing protocols and were stored at −80°C until sent for protein quantification. To reduce batch effects, the samples were shipped together to SomaLogic and randomly distributed across plates. Protein levels were measured using the SomaScan v4.1 platform, an aptamer-based technology that allows for multiplexed protein quantification. The resulting dataset included quantitative measurements of more

than 7,000 aptamers, expressed in relative fluorescence units (RFU). Initial data normalization was carried out by SomaLogic, which applied hybridization controls to address intra-plate variation and median signals for inter-plate adjustments.[22] Additionally, the data were further normalized against an external reference to account for biological variability.[24]

Subsequent quality control (QC) at both the aptamer and individual sample levels was performed using an internally developed protocol.[23] Aptamers were first filtered based on limit of detection (LOD), defined as the mean signal in buffer samples plus two standard deviations. Aptamers with more than 85% of samples below the LOD were excluded. Additional technical filters were then applied, removing aptamers if the maximum absolute difference between calibration and median scale factors across plates exceeded 0.5, or if the median coefficient of variation (CV) across plates was greater than 0.15. Outliers were identified using a 1.5× interquartile range (IQR) threshold on log10-transformed RFU values and were set to missing rather than removed. Following this, sequential two-stage call rate filtering was applied, excluding aptamers and samples with call rates below 65% and subsequently 85%. Aptamers targeting non-human proteins were excluded in the final step. The $\log_{10}$-transformed RFU values were further normalized using a z-score transformation with center and scaling set to true, which ensured they had a mean of 0 and a standard deviation (SD) of 1. After applying all these QC steps, 558 samples (178 Aβ+ and 380 Aβ-) and 6,873 aptamers passed QC in the plasma data. The same quality control and normalization pipeline was applied to the Bio-Hermes data.

2.5 | Positron emission tomography

Knight-ADRC: The amyloid-β (Aβ) PET scans were performed using different tracers, including ^{11}C-Pittsburgh compound-B (PiB) measured in Centiloid units and florbetapir F-18 (FBP). For standardization, amyloid PET data from each tracer were normalized to their reference cerebellar regions in order to obtain SUVRs in a composite of cortical brain areas. To normalize amyloid PET endophenotypes across different tracers, we converted different amyloid imaging measures into $\log_{10}$-normalized z-scores using the "scale" function in base R, with "center" and "scale" set to true. These normalized z-scores were used for dichotomizing Aβ PET into biomarker positive (Aβ+) and negative (Aβ–), as previously described.[25,26] Briefly, defining biomarker positivity and negativity requires the selection of a cut point. We and others[27,28] have demonstrated that it is possible to use a Gaussian mixture model (GMM) to statistically infer that cut-off by relying on hierarchical model-based agglomerative clustering. to dichotomize amyloid PET, applying a z-score threshold of 0.78 (corresponding to a raw value of 33.01) for FBP and 0.643 (corresponding to a raw value of 25.85) for PiB.[26]

Bio-Hermes: Cerebral Aβ deposition was assessed with amyloid PET using the FBP tracer, described in detail elsewhere.[17] For analysis in which a binary cut-off for amyloid positivity was required, the z-score cut-off of 0.71 (corresponding raw value of 62.71) for FBP was selected based on a GMM-based approach, as described earlier.

2.6 | Differential abundance analysis (DAA)

Multiple linear regression models adjusting for baseline age, sex, tracer (in Knight-ADRC), and the first two proteomic principal components (PC1 and PC2) were used to examine associations of proteins with mean cortical Aβ. Because PiB PET in the presence of low or absent Aβ (i.e., Aβ– participants) can reflect tracer kinetics rather than Aβ deposition,[29] we examined how proteins correlated with mean cortical Aβ separately across Aβ+ participants and the total sample. Logistic regression models adjusted for the same covariates were used to examine associations of proteins with dichotomized (Aβ+ vs Aβ–) status. Proteins that passed association with $p < 0.05$ and false discovery rate (FDR) < 0.05 were treated as nominally and FDR significant, respectively.

2.7 | Derivation of amyloid-associated plasma proteomic score and association analyses

To quantify the aggregate effect of replicated amyloid-associated plasma proteins, we constructed a weighted proteomic score (z) based on the 54 proteins that demonstrated concordant directionality and nominal significance in both the Knight-ADRC (discovery) and Bio-Hermes (validation) cohorts. Within each cohort, protein abundances were first standardized to z-scores to ensure comparability across analytes with differing dynamic ranges. In the discovery cohort, we first fit linear regression models relating each of these 54 proteins to continuous amyloid PET burden within Aβ+ individuals, and we used the resulting effect-size estimates βj as weights. For a given individual i, the raw proteomic score was calculated as

$$S_i = \sum_{j \in O_i} \beta_j Z_{ij},$$

where Zij is the standardized abundance of protein j in individual i, and Oi is the set of proteins with non-missing measurements for that individual. To avoid bias from missing values, we normalized this score by the sum of the absolute weights for the observed proteins:

$$S_i^{norm} = \frac{S_i}{\sum_{j \in O_i} |\beta_j|}.$$

The normalized score S_i^{norm} was then z-transformed across individuals to obtain the final proteomic score used in downstream analyses. An analogous cohort-specific score was independently derived in the Bio-Hermes cohort using effect-size estimates generated within that cohort.

Associations between the proteomic score and clinical, cognitive, and biomarker traits were evaluated using linear or logistic regression

models as appropriate. Continuous outcomes included MMSE, CDR-SB, normalized amyloid PET burden, and plasma Aβ42 levels, while clinical AD status was modeled as a categorical outcome. All models were adjusted for age at blood draw, sex, and Apolipoprotien E (*APOE)* genotype. Because the proteomic score was developed to capture inter-individual variability in amyloid burden among Aβ+ participants, primary analyses were conducted within the amyloid-PET-positive subset, with full-cohort analyses performed for comparison. Effect sizes (β), Pearson's correlation coefficient (r) values, and corresponding p values were reported, and statistical significance was assessed using two-sided Wilcoxon rank-sum tests.[30]

2.8 | Unsupervised hierarchical clustering of plasma proteome

To examine global patterns of similarity across diagnostic groups, we performed unsupervised hierarchical clustering on the standardized effect size from the association analysis of identified proteins with different clinical and pathological traits. Effect sizes from the linear (in the case of quantitative trait) and logistic (for binary traits) regression models were divided by their standard error (SE). Hierarchical clustering was carried out using Euclidean distance as the similarity metric and complete linkage as the agglomeration method. Heatmaps with dendrograms were generated to visualize proteomic clustering patterns across different clinical and biomarker traits. All analyses were performed in R (version 4.3.0) using the packages ComplexHeatmap (version 2.16.0) for heatmap visualization and stats for clustering.

2.9 | Pathway enrichment analysis

Functional enrichment analysis was performed separately for each protein cluster using the ClusterProfiler R package (version 4.8.1).[31] Reactome[32] pathway enrichment analysis was performed using the "enrichPathway" function, Gene Ontology (GO)[33] using "EnrichGO," Kyoto Encyclopedia of Genes and Genomes (KEGG)[34] using "enrichKEGG," WiKi pathways[35] using "enrichWP," and the human disease ontology (DO)[36] using "enrichDO." The default universal set of genes served as the reference background for all of the enrichment analyses. Only significantly enriched pathways ($p < 0.05$) were reported. Functional enrichment significance was determined using a hypergeometric test for over-representation.

2.10 | Ethics statement

Ethics approval for the Knight-ADRC was obtained from the Institutional Review Boards (IRBs), and the research was conducted following the approved protocols (WUSTL IRB approval 201109148). Written informed consent was obtained from participants or their family members, and the study design was approved by all participating institutions.

The Bio-Hermes protocol was approved by the central IRB. All participants gave written informed consent prior to participation, and de-identified data were used for analyses.

3 | RESULTS

We analyzed plasma proteomic and amyloid PET data from two independent cohorts separately, comprising a total of 1429 individuals. (Figure 1, Table 1). The discovery cohort from the Knight-ADRC comprised 558 participants (178 Aβ+ and 380 Aβ−), and the Bio-Hermes validation cohort included 871 participants (241 Aβ+ and 630 Aβ−). Plasma proteins were quantified with the SomaScan version 4.1 platform, yielding measurements for approximately 7000 analytes, and were integrated with quantitative amyloid PET values obtained using FBP and PiB tracers. We next examined plasma proteomic signatures associated with amyloid load across all individuals (Aβ+ and Aβ−) and only those that were Aβ+, evaluated their relationships with clinical and fluid biomarker traits, developed a proteomic score to predict amyloid burden, and investigated the underlying biology through clustering and pathway enrichment analyses.

3.1 | Plasma proteomic signatures of amyloid PET

We first assessed associations between continuous amyloid PET measures and plasma protein levels in the Knight-ADRC cohort ($n = 558$) using linear regression models adjusted for age, sex, tracer, and the first two proteomic principal components. Of the 6870 protein analytes profiled, 470 were nominally associated ($p < 0.05$) with amyloid load, and 14 remained significant after multiple testing correction (FDR < 0.05; Figure 2A and Table S1). These proteins included previously implicated markers of neurodegeneration (e.g., FOXO1, SPC25, and LRRN1) as well as putative novel candidates (e.g., CPLX2, CTF1, TBCA). To further characterize the proteomic correlates of amyloid pathology, we analyzed amyloid PET as a dichotomous trait (Aβ+ vs Aβ−; Figure 2B). This comparison yielded 895 nominally associated proteins, of which 53 passed FDR correction. Many of the top signals overlapped with those from the continuous models for all individuals, reinforcing their relevance across different trait definitions; SPC25, CPLX2, CTF1, and FOXO1 were among the most consistently associated proteins.

Because our primary goal was to identify proteins linked to higher amyloid burden, we next repeated the analysis in Aβ+ individuals only ($n = 178$; Figure 2C). In this subset, 454 proteins showed nominal associations ($p < 0.05$) with continuous amyloid PET. Proteins such as C1orf185, LMNB1, and DNAJC19 showed the strongest positive correlations with amyloid load, whereas VPS29, TGIF2, and DLL3 were negatively associated. We then compared the sets of nominally associated proteins across the three analytic strategies (continuous in all participants, dichotomous Aβ+ vs Aβ−, and continuous in Aβ+ only; Figure S1A). Twenty proteins were shared across all models, defining a core group of amyloid-related plasma markers, whereas larger

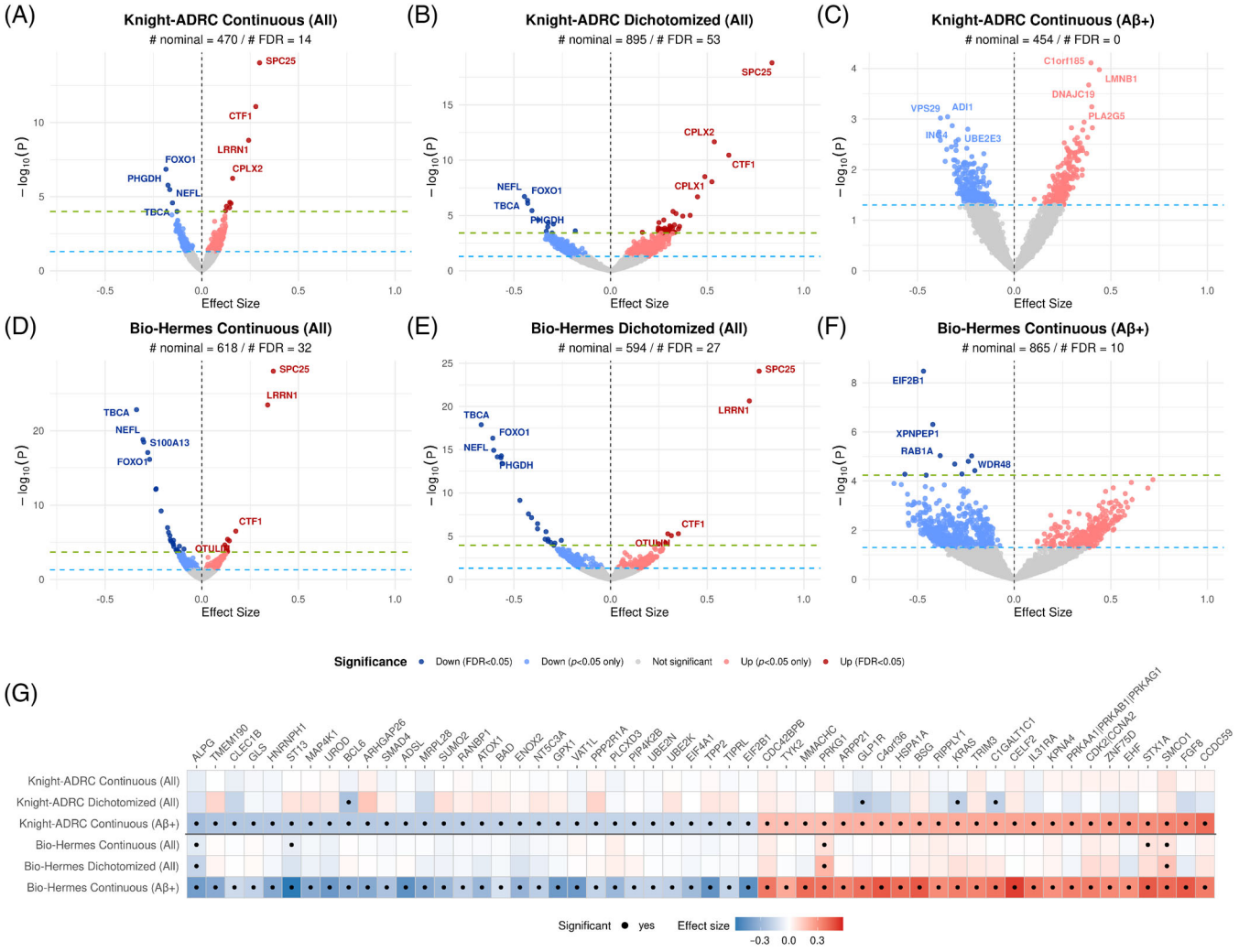

FIGURE 2 Plasma proteomic associations with amyloid PET in discovery and validation cohorts. (A–C) Associations between plasma protein levels and amyloid PET in the discovery cohort (Knight-ADRC). Each point in the volcano plots represents one of approximately 7000 proteins, plotted by effect size (*x*-axis) and significance ($-\log_{10}$ FDR or *p* value, *y*-axis). Proteins positively associated with amyloid load are shown in red; negatively associated proteins are shown in blue. (A) Continuous amyloid PET across all participants identified 470 nominally associated proteins, including 14 that passed FDR correction. (B) Dichotomized amyloid PET status (Aβ+ vs Aβ−) across all participants identified 895 nominally associated proteins, of which 53 remained significant after false discovery rate (FDR) correction. (C) Continuous amyloid PET among Aβ+ individuals identified 454 proteins with nominal associations. (D–F) Replication of amyloid-associated proteomic signatures in the Bio-Hermes validation cohort. (D) Associations with continuous amyloid PET in all participants; (E) dichotomized amyloid status in all participants; (F) continuous amyloid PET in Aβ+ individuals. (G) Heatmap of effect size for 54 proteins that showed robust association with continuous amyloid PET in Aβ+ individuals across discovery (Knight-ADRC) and validation (Bio-Hermes) cohorts.

subsets were unique to individual approaches, indicating that continuous and dichotomous PET measures captured complementary aspects of amyloid-linked proteomic variation. On this basis, subsequent analyses focused on proteins associated with continuous amyloid PET within Aβ+ individuals, to emphasize proteomic changes related to elevated amyloid burden in the brain.

To evaluate the reproducibility of these associations, we carried out independent validation in the Bio-Hermes cohort.[17] Using the same regression framework, we modeled protein associations with three amyloid PET traits: continuous and dichotomized values in all participants and continuous values in Aβ+ individuals. In Bio-Hermes (n = 871), 32 and 27 proteins were significantly associated (FDR < 0.05) with continuous and dichotomized amyloid PET, respectively (Figure 2D,E). Several proteins identified in the Knight-ADRC cohort, including SPC25, LRRN1, CTF1, CPLX2, and FOXO1, showed concordant and significant associations in this independent validation cohort. When analyses were restricted to only Aβ+ individuals (n = 241), 10 proteins remained significant after FDR correction and an additional 855 were nominally associated (Figure 2F); among the FDR-significant proteins, EIF2B1, ST13, and TPP2 also showed

nominal associations with concordant effect size directions in Knight-ADRC discovery cohort. Across all three analytic strategies in Bio-Hermes, 66 proteins were consistently associated with amyloid PET (Figure S1B), regardless of how the PET trait was defined.

We next examined effect-size concordance between cohorts to evaluate the robustness of identified associations (Figure S2). For continuous amyloid PET in all individuals, effect sizes for proteins nominally associated in Bio-Hermes were strongly correlated with those from Knight-ADRC (Pearson's correlation coefficient $r > 0.6$, $p = 4.2\times10^{-06}$), increasing to $r = 0.97$ ($p < 1.2\times10^{-12}$) when restricted to proteins significant at FDR < 0.05 in Bio-Hermes. For analyses limited to Aβ+ individuals, 290 of 436 overlapping proteins (67%) showed concordant-effect directions, with an overall effect-size correlation of 0.32 ($p < 2.2\times10^{-16}$; Table S2). This correlation improved to 0.76 ($p < 2.2\times10^{-16}$) and 0.98 ($p < 1.2\times10^{-13}$) when only nominally and FDR-significant proteins in Bio-Hermes were considered, respectively. Of these 290 overlapping proteins, 54 were also nominally associated in the Bio-Hermes cohort, indicating a subset of robust amyloid-related markers with consistent effects across independent samples (Figure 2G).

As a sensitivity analysis, we evaluated associations between plasma proteins and tau-PET measures in the Knight-ADRC cohort. Although tau PET and amyloid PET proteomic signatures showed moderate concordance in effect sizes (maximum $r = 0.69$; concordance = 81%), the overlap of nominally associated proteins was limited (6% to 20% across tau-PET analyses), supporting the relative specificity of the amyloid-associated proteomic signals (Figure S3). Together, these results support a reproducible plasma proteomic signature of cerebral amyloid burden across independent cohorts and provide a robust basis for downstream mechanistic and translational analyses.

3.2 | Plasma proteins define clinically relevant molecular heterogeneity within Aβ+ individuals

To prioritize biologically robust signals linked to cerebral amyloid pathology, we focused on the 54 plasma proteins that showed the same direction of effects and nominal significance in both the Knight-ADRC and Bio-Hermes cohorts. In limiting our analyses to proteins that replicated across these independent samples, we aimed to enrich for shared amyloid-related biology rather than cohort-specific noise. The replicated panel included regulators of proteostasis and cellular stress (e.g., HSPA1A, UBE2K, SUMO2), kinase and metabolic signaling (e.g., PRKAA1/PRKAB1/PRKAG1, KRAS, MAP4K1, BAD), immune mediators (e.g., TYK2, IL-31RA, BCL6), and synaptic or neuronal components (e.g., STX1A, ARPP21, PRKG1), suggesting coordinated perturbation of intracellular signaling, immune, and protein quality-control pathways.

Using effect-size estimates from Knight-ADRC, we constructed a weighted amyloid-associated proteomic score (z) and examined its clinical relevance. Because this score was designed to capture variation in amyloid burden among Aβ+ individuals, downstream analyses were performed primarily in the Aβ+ subset ($n = 178$), where variation reflected disease severity rather than presence versus absence of amyloid. Within this group, higher proteomic scores were associated with greater clinical impairment: Scores were higher in AD compared with cognitively normal individuals ($p = 0.02$; Figure 3A) and increased across global CDR categories from 0 to 1 ($p = 0.02$; Figure 3B). When stratified by combined CSF Aβ_{42} (A) and hyperphosphorylated tau$_{181}$ (T) status, the highest scores were observed in A^+T^+ individuals ($p = 0.03$), indicating that the proteomic signature tracked with more advanced biomarker-defined disease stage (Figure 3C).

Consistent with these group-wise differences, higher proteomic scores tended to relate to worse cognition and function among Aβ+ individuals, showing a trend toward lower MMSE ($r = -0.13$, $p = 0.08$; Figure 3D) and a significant positive association with CDR-Sum of Boxes (CDR-SB) ($r = 0.19$, $p = 0.01$; Figure 3E). Effect-size estimates were directionally consistent for associations between the proteomic score and clinical/biomarker outcomes (Figure 3F). In contrast, associations were attenuated and not statistically significant when the score was evaluated in the full Knight-ADRC cohort ($n = 558$), consistent with dilution of amyloid-related signal by Aβ− individuals (Figure S4A–D). Pathway enrichment of the 54 proteins demonstrated over-representation of PI3K-Akt/mTOR signaling, cell-cycle and kinase complexes, interferon and immmue signaling, and autophagy-related processes (Figure S4E and Table S3), underscoring the biological coherence of this replicated plasma signature and its relevance to clinical heterogeneity emerging after amyloid positivity.

In parallel, we generated a cohort-specific proteomic score in Bio-Hermes using the same 54 proteins and their effect-size estimates from that cohort. Higher values of this validation score were associated with clinical AD diagnosis and higher normalized amyloid PET levels and were inversely related to MMSE performance and plasma Aβ42 concentrations (Figure S4F–H). The concordant direction and pattern of trait associations across both cohorts support the robustness of this proteomic signature as a biologically meaningful correlate of amyloid-related disease severity. Notably, in the Knight-ADRC cohort where *APOE* genotype was available, the associations between the proteomic score and clinical and biomarker traits were not modified by *APOE* ε4 status (Figure S5), suggesting that this signature captures amyloid-related molecular variation that is largely independent of *APOE*-driven genetic risk.

3.3 | Association of amyloid-related plasma proteins with clinical and molecular AD traits

To investigate the broader biological and clinical relevance of amyloid-associated proteins, we related the 454 proteins identified in Aβ+ individuals to a panel of AD biomarkers and clinical measures. These traits included CSF Aβ42, Aβ40, the Aβ42/Aβ40 ratio, hyperphosphorylated tau$_{181}$ (p-tau), total tau (Tau), CSF AT status (A^+T^+ vs A^-T^-), standardized CDR, binarized CDR status (CDR = 0 vs CDR > 0), CDR-SB, clinical diagnosis (AD vs control), MMSE, age at onset, and age-at-onset group (early vs late onset using a 65-year cut-off). We first focused on the 54 replicated proteins that showed concordant, nominal associations with amyloid load in both cohorts. Several proteins,

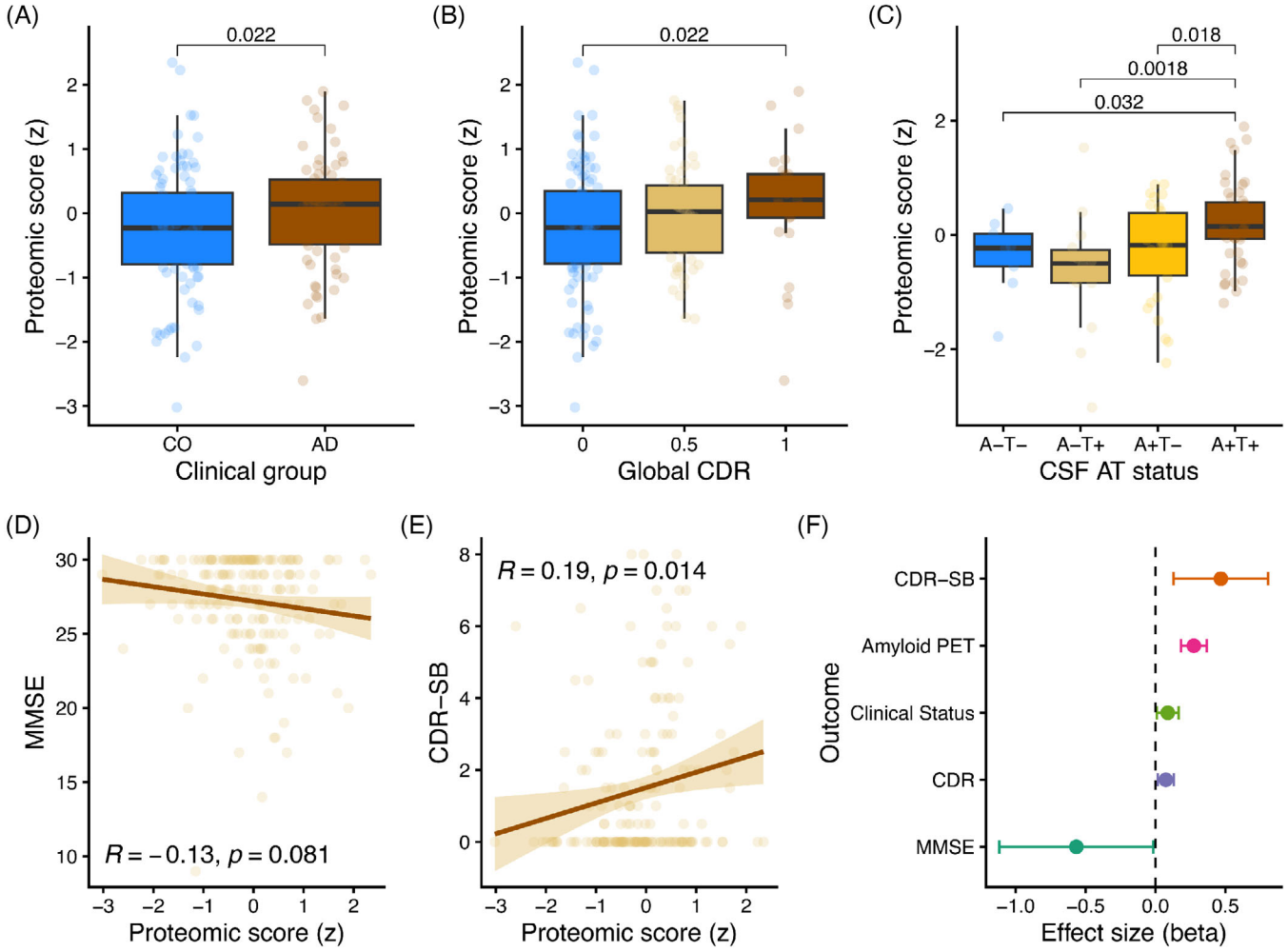

FIGURE 3 Amyloid-associated plasma proteomic score stratifies clinical severity within amyloid-positive individuals. Association of the 54-protein amyloid-associated proteomic score (z) with clinical and cognitive outcomes in amyloid-positive individuals ($n = 178$). (A) Distribution of the proteomic score across clinical groups (cognitively normal [CO] vs Alzheimer's disease [AD]). (B) Proteomic score across global Clinical Dementia Rating (CDR) categories. (C) Proteomic score stratified by combined CSF $A\beta_{42}$ (A) and hyperphosphorylated tau_{181} (T) status, showing the highest levels in A^+T^+ individuals. (D) Association between proteomic score and MMSE. (E) Association between proteomic score and CDR-SB. Lines represent linear regression fits with 95% confidence intervals. (F) Forest plot summarizing standardized effect sizes (beta coefficients ± 95% CI) for associations between the proteomic score and clinical/biomarker outcomes.

such as VAT1L and IL-31RA, were associated with clinical diagnosis, whereas others, including CELF2, TYK2, and PRKAA1, showed consistent relationships across multiple clinical and cognitive measures (Figure 4A).

We then extended these analyses to all 454 proteins to identify broader groups of proteins linked to shared clinical and biomarker profiles. Hierarchical clustering of trait-association effect sizes revealed distinct modules of proteins with correlated patterns of association (Figure 4B and Table S1). The Gap statistics (k)[37] and total within-cluster sum of squares[38] supported a five-cluster solution (Figure S6). Notably, some clusters were enriched for proteins showing concordant associations with amyloid and tau biomarkers, while others were more closely aligned with measures of clinical severity such as MMSE and CDR. For example, proteins in Cluster 1 (84 proteins) showed positive associations with higher CDR scores and earlier age at onset, consistent with a molecular profile of more aggressive or early-presenting disease. Proteins in Cluster 2 (51 proteins) were also enriched for early-onset cases but showed comparatively weaker associations with measures of clinical severity, suggesting trajectories of earlier yet less rapidly progressive pathology. In contrast, proteins in Cluster 3 (59 proteins) exhibited inverse associations with both pathology and cognitive decline, compatible with a resilience- or protection-related signature. Cluster 4 proteins (80 proteins) were characterized by later onset but stronger associations with worsening CDR and CDR-SB, indicating a profile of rapid deterioration once symptoms emerge. Finally, Cluster 5 (180 proteins) showed subtle but broad positive associations across multiple traits, pointing to involvement of more generalized systemic processes, including neurodegenerative and inflammatory activity. Together, these findings indicate that amyloid-associated plasma proteins do not form a single homogeneous signal but instead resolve into biologically meaningful modules that map onto distinct clinical trajectories, spanning early versus late onset,

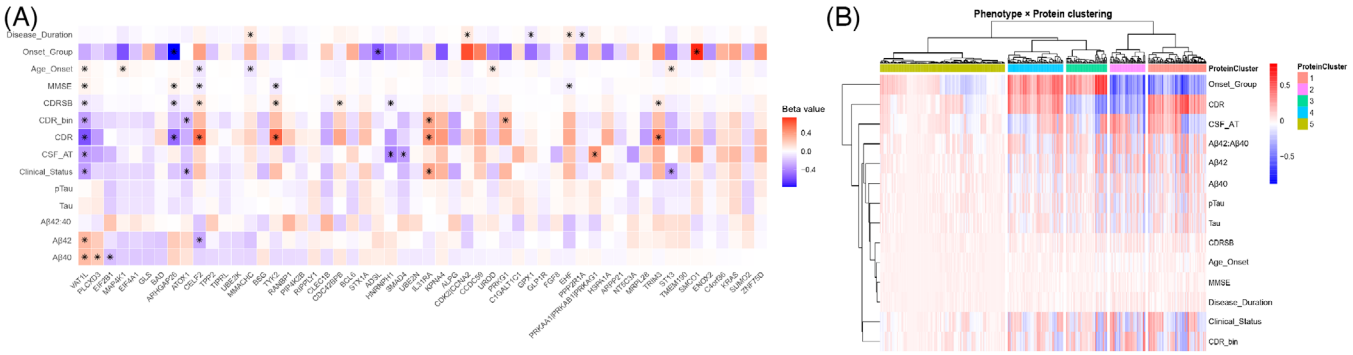

FIGURE 4 Trait associations and clustering of amyloid-related plasma proteins. (A) Heatmap of effect sizes for associations between the 54 replicated amyloid-related proteins and Alzheimer's disease biomarkers and clinical traits in the Knight-ADRC cohort. Traits include CSF Aβ42, Aβ40, Aβ42/Aβ40 ratio, hyperphosphorylated tau$_{181}$ (pTau), total tau (Tau), CSF AT status (A^+T^+ vs A^-T^-), standardized CDR, binarized CDR (CDR = 0 vs CDR > 0), CDR-Sum of Boxes (CDR-SB), clinical diagnosis, Mini-Mental State Examination (MMSE), age at onset, and age-at-onset group (early vs late onset, 65-year cut-off). Asterisks denote nominally significant associations ($p < 0.05$). (B) Heatmap of effect sizes (β coefficients) for associations between the full set of 454 amyloid-associated proteins and the same biomarker and clinical traits in Aβ+ individuals. Hierarchical clustering of proteins and traits revealed five protein clusters (colored bars at the top) with correlated association patterns, as determined by gap statistics and within-cluster sum-of-squares criteria. Red and blue indicate positive and negative associations, respectively. These clusters represent coherent molecular modules that capture coordinated relationships among amyloid, tau, and clinical measures.

relatively benign versus high-risk progression, and putative resilience in AD.

3.4 | Pathway enrichment analysis

To better understand the biology underlying the five protein clusters derived from the trait-association heatmap, we performed pathway enrichment analyses using GO,[33] KEGG,[34] Reactome,[32] WikiPathways,[35] and DO[36] databases. Distinct and biologically coherent enrichment profiles emerged for each cluster, indicating that they represented separable molecular programs that may contribute to different clinical trajectories among Aβ+ individuals (Figure 5 and Table S4).

Cluster 1 (C1), which was positively associated with higher CDR scores and earlier disease onset, was enriched for fibroblast growth factor (FGF) signaling, cytokine activity, and postsynaptic organization, including FGF2, interleukin (IL)-6R, IL-17C, IL-25, and NPTX2. Enrichment for pathways such as *response to fibroblast growth factor stimulus* and *signaling by interleukins* points to coordinated activation of inflammatory and growth factor–mediated cascades,[39,40] consistent with glial activation and neuronal stress responses reported in rapidly progressing AD.[40] The presence of synaptic and neuronal proteins such as STX1A, NPTX2, and SIRT2 further supports a role for synaptic dysfunction and neurodegenerative signaling in this high-risk cluster.[10,41]

Cluster 2 (C2), associated with earlier onset but comparatively slower progression, showed enrichment for immune-modulatory and cell-signaling pathways, including *T-cell receptor signaling* (UBE2D1, UBE2V1, UBE2N) and *mTOR signaling* (EIF4E, YWHAB). These pathways are implicated in neuroimmune interactions and regulation of protein translation, processes that are relevant to neurodegeneration.[42,43] Additionally, IL-17 *signaling* and *prostaglandin signaling pathways* (IL-17A, IL-17F) were also prominent, suggesting cytokine-driven neuroinflammation and vascular contributions.[44] DO results further connected C2 proteins to macular degeneration, vascular dementia, and both Alzheimer's and tauopathy, demonstrating a direct relationship of this cluster with canonical neurodegenerative phenotypes.

Cluster 3 (C3) showed the opposite clinical pattern to C1, with later onset and lower CDR scores, consistent with a resilience-associated signature. Enriched pathways included *positive regulation of leukocyte activation* (TNFSF4, BAD, FCGR3A, HAVCR1, IL-12RB1, THY1), *memory T-cell differentiation* (TNFSF4, IL-12RB1), and *neuropeptide activity* (ADCYAP1, PNOC). Several C3 proteins (FMR1, THY1, APBB2, PNOC) are involved in distal axon biology and synaptic plasticity, supporting a role for neuronal resilience.[45] Reactome terms highlighted downregulation of transforming growth factor beta (*TGF-β) receptor signaling* (STUB1, BAMBI, USP15), a pathway that restrains glial activation and chronic neuroinflammation,[46] and *p53-Dependent G1 DNA Damage Response* (PSMC3, CDK2, CCNA2), which are linked to cellular stress resistance and neuroprotection.[47] Together, these features suggest that C3 captures adaptive immune and neuropeptide-mediated mechanisms that may protect against amyloid-related decline.

Cluster 4 (C4) was enriched for *vesicle lumen*, *lipoprotein particle metabolism*, *cell chemotaxis*, *sphingolipid biosynthetic process*, and *protein ubiquitination*. Proteins such as SAA1, PON1, and MSR1 are implicated in lipoprotein remodeling and innate immune activation,[48,49] while PPM1L, SPTLC1, and SIRT3 pointed to the regulation of mitochondrial and membrane lipid homeostasis.[50,51] Chemotaxis-related proteins (GAS6, CXCL3, RAB13) and ubiquitination components (VCP, UBE2V2, UBE2K) suggested links between immune recruitment, proteostasis, and neurodegeneration.[52,53] Overall, C4 reflects a lipid–immune–proteostasis axis that may exacerbate metabolic stress and neuroinflammatory imbalance, aligning with the rapid clinical decline observed in this cluster.

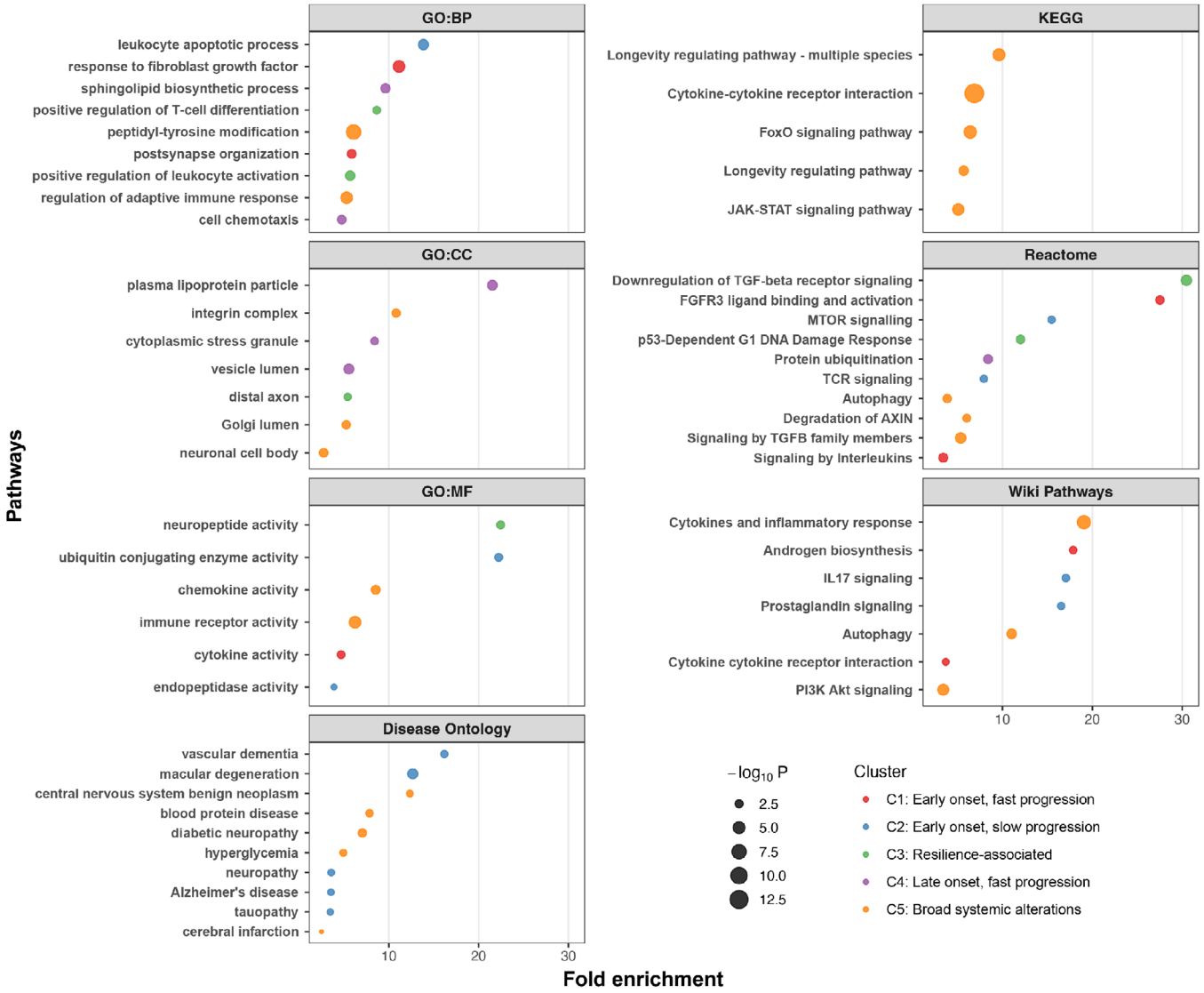

FIGURE 5 Pathway enrichment analysis of amyloid-associated plasma protein clusters. Dot plots display significant Gene Ontology (GO; including BP, CC, MF), KEGG, Reactome, Wiki Pathways, and Disease Ontology (DO) enrichments for plasma protein clusters ($n = 5$) associated with continuous amyloid PET in Aβ+ individuals. Proteins were grouped into clusters based on clinical trait associations, and pathway enrichment was performed for each cluster. Dot size denotes the significance of enrichment (−log10 p), while color indicates cluster identity.

Cluster 5 (C5) displayed broad yet coordinated enrichment of immune, metabolic, and intracellular signaling pathways, consistent with systemic inflammation and neurodegenerative stress responses. Key processes included *adaptive immune regulation*, *chemokine and cytokine-mediated signaling*, *autophagy*, and *FoxO/PI3K–Akt pathways*. Multifunctional proteins such as TGFB1, IL-12A/B, IL-4, PRKAA1, and PRKAG1 connect this cluster to inflammatory and longevity-regulating mechanisms that likely reflect compensatory responses to accumulating neural injury.[54,55] Additional enrichment for neurotrophic and metabolic regulators within PI3K–Akt signaling (NGF, FGFR3, INS, and PPP2R1A) underscores cross-talk between neuronal survival, oxidative stress control, and energy homeostasis.[56] DO terms related to diabetic neuropathy, hyperglycemia, and vascular disorders indicate that C5 also captures systemic metabolic and vascular pathology that can heighten vulnerability to neurodegeneration.

Taken together, these pathway results show that the five amyloid-related plasma protein clusters represent biologically distinct molecular programs that align with their clinical phenotypes. The association of C1 with growth factor signaling (FGF2, GALNT3) and synapse organization (STX1A, NPTX2) corresponds to its link with aggressive disease progression driven by neuroinflammation and synaptic dysfunction. Enrichment of C2 for immune modulation (ADAM17, IL-17A/F) and mechanistic target of repamycin (mTOR) / T-cell receptor (TCR) signaling (YWHAB, UBE2D1) defines an early-onset but slower-progressing profile involving neuroimmune and vascular processes. The protective C3 is characterized by immune regulation (TNFSF4, IL-12RB1), neuropeptide activity (ADCYAP1, PNOC), and stress response (PSMC3, CDK2) pathways, suggesting molecular resilience through adaptive immunity and neuroprotection. Involvement of C3 proteins in lipid metabolism (PPM1L, SIRT3), vesicular transport (SAA1, CXCL3),

and proteostasis (VCP, UBE2V2) highlights metabolic and immune dysregulation that may drive rapid clinical decline. Finally, C5 integrates systemic inflammation (TGFB1, IL-12A/B), autophagy (PRKAA1, PRKAG1), and neurotrophic signaling (NGF, PPP2R1A) through FoxO and PI3K-Akt pathways, reflecting widespread neurodegenerative stress and metabolic vulnerability. Collectively, these pathway enrichments provide mechanistic insights into the heterogeneous proteomic states that underlie distinct clinical trajectories in Aβ+ individuals, underscoring the value of cluster-based molecular stratification.

4 | DISCUSSION

Plasma is an accessible biofluid that can capture both systemic and central nervous system (CNS)–related biology, offering a practical window into molecular alterations associated with AD. Yet, our understanding of robust, amyloid-specific changes within the plasma proteome remains limited. Previous plasma and CSF proteomic studies identified candidate markers of amyloidosis and neurodegeneration, but most profiled a limited subset of proteins and relied on dichotomous case–control or amyloid status contrasts, which can obscure continuous relationships across the disease spectrum.[12–15] Only a few studies examined individuals across the full amyloid continuum, and even fewer focused specifically on Aβ+ individuals to identify proteins that track with continuous amyloid load,[7] a key step toward understanding biological heterogeneity and pathogenic mechanisms. Although established biomarkers such as plasma p-tau217 provide sensitive measures of AD-related pathology, they do not fully capture the broader systemic and molecular processes that contribute to disease progression.[57] In parallel, as anti-Aβ therapies increasingly target preclinical or asymptomatic individuals,[58] there is a growing need for complementary blood-based biomarkers that can stratify individuals by risk and enable non-invasive, cost-effective monitoring of disease progression and therapeutic response.

In this study, we integrated quantitative amyloid PET with large-scale plasma proteomics across two independent cohorts (Knight-ADRC and Bio-Hermes, $n = 1429$) to identify reproducible amyloid-associated plasma proteins, relate them to clinical and molecular endophenotypes, and delineate their underlying biology through data-driven clustering and pathway enrichment (Figure 1). Proteome-wide analyses revealed that hundreds of circulating proteins track with amyloid PET burden (Figure 2 and Table S1), recapitulating previously reported markers such as SPC25,[12–14] LRRN1,[12,14] and FOXO1,[12,14] as well as novel candidates including CPLX1, TINAGL1, and DLD, which are linked to synaptic regulation,[59] extracellular matrix remodeling,[60] and cellular metabolism,[61] respectively. Restricting analyses to Aβ+ individuals further refined this landscape, nominating proteins specifically associated with higher cerebral amyloid load, including phosphatase-related (PPP2R1A),[62] synaptic (STX1A, VPS29),[12,63] stress-response (HSPA1A, SUMO2),[64,65] and ubiquitin-pathway proteins (UBE2K, UBE2N), that have been implicated in cognition, neuropathology, and AD risk. Importantly, replication in the independent Bio-Hermes cohort confirmed 54 proteins with concordant directions of effect, increasing confidence in the robustness of these associations despite differences in sample composition and statistical power. Together, these findings indicate that plasma proteomics can capture both broad proteome-wide variation associated with amyloid pathology and more specific signals within Aβ+ individuals, complementing CSF and imaging biomarkers. Although effect sizes varied between cohorts even with similar platforms and z-score scaling, directional consistency among top-ranked proteins suggests underlying biological convergence. These quantitative discrepancies likely reflect differences in sample composition, statistical power, and cohort heterogeneity, underscoring the biological and technical complexity of amyloid-associated plasma signatures and highlighting the importance of harmonized study designs and larger samples for reproducible validation.

Building on these associations, we derived an amyloid-associated plasma proteomic score (z) that showed clinically meaningful associations specifically within Aβ+ individuals, whereas no significant links were observed across the full cohort (Figure 3 and Figure S3). This stage-dependent pattern is consistent with current AD biomarker models, in which amyloid accumulation represents an early initiating event and downstream molecular and clinical heterogeneity emerges after pathological thresholds are exceeded.[2,66] Because the score was derived to capture inter-individual variability in amyloid burden among Aβ+ participants, its associations with CDR-SB, MMSE, and clinical diagnosis are most appropriately interpreted within this subgroup. Inclusion of Aβ− individuals likely dilutes these effects, as amyloid-driven biological responses may not yet be engaged, mirroring observations for tau PET and plasma p-tau measures that show their strongest clinical correlations after amyloid positivity.[67,68] The enrichment of constituent proteins in pathways related to PI3K–Akt/mTOR signaling (PRKAA1, KRAS), kinase regulation (MAP4K1, PPP2R1A), interferon-mediated immune responses (BCL6, IL-31RA), and proteostasis (HSPA1A, UBE2K) provides biological context for these associations, implicating processes central to metabolic regulation, innate immune activation, and protein quality control that are increasingly recognized in AD pathophysiology.[69,70] The convergence of these pathways within a replicated plasma signature suggests that the proteomic score we developed may index coordinated systemic responses to amyloid-related cellular stress that shape clinical expression. Although several associations were modest in magnitude, the consistency in direction and trait relationships across both cohorts supports the interpretation that this signature captures biologically meaningful heterogeneity within the Aβ+ stage.

Beyond summarizing amyloid burden, the broader set of amyloid-associated proteins revealed distinct molecular and clinical substructures. Clustering 454 amyloid-related proteins according to their association patterns with established AD biomarkers (e.g., CSF Aβ42, p-tau) and cognitive measures (CDR and MMSE) yielded five coherent modules (C1–C5) that reflected differing patterns of pathology, age at onset, and cognitive decline (Figure 4). C1, associated with earlier onset and higher CDR, was enriched for growth factor signaling (FGF2, GALNT3), cytokine activity (IL-6R, IL-17C), and synaptic proteins (STX1A, NPTX2), aligning with prior work implicating neuroinflamma-

tion and synaptic dysfunction in more aggressive disease courses.[39,71] C2 showed enrichment for immune pathways and mTOR/T-cell receptor signaling (ADAM17, IL-17A/F, YWHAB), consistent with studies linking peripheral immune remodeling and specific cytokine axes to slower clinical progression.[43,44] The C3 cluster, which was associated with later onset and lower CDR, was enriched for immune regulation and neuropeptide activity and contained key synaptic proteins (THY1, FMR1) and neuropeptides (PNOC, ADCYAP1) that are involved in synaptic plasticity,[72] stress modulation, and neuroprotection,[73] consistent with a putative resilience-related program. C4, characterized by lipid metabolism and proteostasis proteins (SAA1, VCP), mirrors evidence connecting altered lipid handling, mitochondrial function, and protein quality control to neurodegeneration and more rapid decline.[49,74] Finally, C5 reflected systemic inflammation, autophagy, and neurotrophic signaling (TGFB1, PRKAA1, NGF), echoing the role of AMPK–FoxO and PI3K–Akt pathways in stress and energy homeostasis.[55,56] Taken together, these clusters highlight mechanistic heterogeneity among Aβ+ individuals and suggest that distinct plasma proteomic programs may underlie differences in age at onset, rate of progression, and potentially treatment response.

While our findings are robust, several limitations merit consideration. First, sample sizes within the Aβ+ subsets of both cohorts limited power for stringent multiple-testing correction, particularly for weaker effects, and the largely cross-sectional design precludes causal inference. Future work incorporating longitudinal plasma proteomics, multi-omics integration, and larger, harmonized cohorts will be important to characterize dynamic changes in amyloid-related protein networks and to evaluate their prognostic value. Second, although plasma offers a minimally invasive window into CNS-related processes, circulating protein levels are influenced by systemic factors such as inflammation, metabolic status, medications, and comorbid conditions, which may confound associations with cerebral amyloid load.[5,6] Third, the cohorts analyzed here were predominantly of European ancestry and recruited through specialized centers, which may limit generalizability to more diverse and community-based populations. Fourth, pathway and clustering inferences rely on current annotation resources and may not capture context-specific interactions or novel functions, emphasizing the need for experimental validation of key proteins and implicated pathways.[75] Finally, although amyloid-associated proteomic signals were largely concordant across cohorts, differences in effect sizes likely reflect variation in sample size of Aβ+ individuals (229 in Knight-ADRC vs 325 in Bio-Hermes) and imaging protocols (PiB and FBP in Knight-ADRC vs FBP in Bio-Hermes). Nonetheless, the consistent directionality of effect sizes and replication of key proteins across both cohorts support the robustness of the underlying biological signals.

In summary, this study defines a reproducible plasma proteomic signature of cerebral amyloid load, delineates biologically distinct protein clusters linked to clinical and biomarker variation, and illustrates the potential of peripheral proteomics for mechanistic insights and molecular stratification in AD. By connecting systemic protein signatures to central amyloid pathology and downstream clinical outcomes, our findings provide a framework for incorporating plasma biomarkers into precision medicine strategies that aim to stage disease, identify high-risk or resilient subgroups, and monitor therapeutic effects in individuals along the Alzheimer's continuum.

AUTHOR CONTRIBUTIONS

Muhammad Ali: Conceptualization, supervision, formal analysis, validation, visualization, project management, writing – original draft, writing – review and editing. Yike Chen: Data pre-processing and quality check, formal analysis, visualization, review and editing. Carlos Cruchaga: Conceptualization, funding acquisition, supervision, review and editing. John C. Morris, David M. Holtzman: Funding acquisition, project administration, review and editing. Jigyasha Timsina, Menghan Liu, Michael R. Duggan: Data pre-processing and quality check. Michael R. Duggan, Ying Xu, Daniel Western, Katherine Gong, John Budde, Suzanne E. Schindle, Tammie L.S. Benzinger, Brian A. Gordon, Mahdi Moqri, Laura Ibanez, and Keenan A. Walker: Data curation, review and editing.

ACKNOWLEDGMENTS

We extend our gratitude to all the participants and their families, as well as the involved cohorts, institutions, and their dedicated staff. This work was supported by access to equipment made possible by the Hope Center for Neurological Disorders, the Neurogenomics and Informatics Center (NGI: https://neurogenomics.wustl.edu/), and the Departments of Neurology and Psychiatry at Washington University School of Medicine. This work was supported by grants from the National Institutes of Health (R01AG044546 (CC), P30AG066444 (DMH), RF1AG053303 (CC), RF1AG058501 (CC), U01AG058922 (CC), the Chan Zuckerberg Initiative (CZI), the Michael J. Fox Foundation (CC), the Alzheimer's Association Zenith Fellows Award (ZEN-22-848604, awarded to CC), and an Anonymous foundation. The recruitment and clinical characterization of research participants at Washington University were supported by NIH P30AG066444 (DMH), P01AG03991(JCM), and P01AG026276(JCM). This research was supported [in part] by the Intramural Research Program of the National Institutes of Health (NIH). The contributions of the NIH author(s) are considered Works of the United States Government. The findings and conclusions presented in this paper are those of the author(s) and do not necessarily reflect the views of the NIH or the U.S. Department of Health and Human Services.

CONFLICT OF INTEREST STATEMENT

CC has received research support from GSK and EISAI. CC is a member of the scientific advisory board of Circular Genomics and owns stock in the company. CC is a member of the scientific advisory board of ADmit. The other authors declare that they have no conflicts of interest. Author disclosures are available in the Supporting Information.

DATA AVAILIABILITY STATEMENT

Plasma proteomic data from Knight-ADRC participants are available through the Knight-ADRC data request portal (https://live-knightadrc-washu.pantheonsite.io/professionals-clinicians/request-center-resources/). Requests are subject to review to ensure compliance

with patient confidentiality. Additional information about available data and study protocols can be found at https://knightadrc.wustl.edu. Anonymized Bio-Hermes data not published within this article may be shared upon request from qualified investigators. Researchers who wish to use Bio-Hermes data are encouraged to develop a pre-analysis plan that can be submitted for approval through Alzheimer's Disease Data Initiative portal (https://discover.alzheimersdata.org/).

CODE AVAILABILITY

The code used for the proteomics analyses is publicly available on GitHub (https://github.com/muhammed-ali/AlzDem_2026_AmyloidPET_Proteomics).

CONSENT STATEMENT

This study was approved by the Institutional Review Board of Washington University School of Medicine in St. Louis. Written informed consent was obtained from all participants or their legally authorized representatives.

CONSENT FOR PUBLICATION

The manuscript's contents have been approved by all the co-authors, and they have provided consent for its publication.

ORCID

Muhammad Ali https://orcid.org/0000-0002-1399-6631

REFERENCES

1. Scheltens P, De Strooper B, Kivipelto M, et al. Alzheimer's disease. *Lancet*. 2021;397:1577-1590. doi:10.1016/S0140-6736(20)32205-4
2. Hansson O. Biomarkers for neurodegenerative diseases. *Nat Med*. 2021;27:954-963. doi:10.1038/s41591-021-01382-x
3. Frisoni GB, Hansson O, Nichols E, et al. New landscape of the diagnosis of Alzheimer's disease. *Lancet*. 2025;406:1389-1407. doi:10.1016/S0140-6736(25)01294-2
4. Heo G, Xu Y, Wang E, et al. Large-scale plasma proteomic profiling unveils diagnostic biomarkers and pathways for Alzheimer's disease. *Nat Aging*. 2025;5:1114-1131. doi:10.1038/s43587-025-00872-8
5. Walker KA, Chen J, Zhang J, et al. Large-scale plasma proteomic analysis identifies proteins and pathways associated with dementia risk. *Nat Aging*. 2021;1:473-489. doi:10.1038/s43587-021-00064-0
6. Ali M, Erabadda B, Chen Y, et al. Shared and disease-specific pathways in frontotemporal dementia and Alzheimer's and Parkinson's diseases. *Nat Med*. 2025;31:2567-2577. doi:10.1038/s41591-025-03833-1
7. Pichet Binette A, Gaiteri C, Wennström M, et al. Proteomic changes in Alzheimer's disease associated with progressive Aβ plaque and tau tangle pathologies. *Nat Neurosci*. 2024;27:1880-1891. doi:10.1038/s41593-024-01737-w
8. Tijms BM, Vromen EM, Mjaavatten O, et al. Cerebrospinal fluid proteomics in patients with Alzheimer's disease reveals five molecular subtypes with distinct genetic risk profiles. *Nat Aging*. 2024;4:33-47. doi:10.1038/s43587-023-00550-7
9. Kirsher DY, Chand S, Phong A, Nguyen B, Szoke BG, Ahadi S. Current landscape of plasma proteomics from technical innovations to biological insights and biomarker discovery. *Commun Chem*. 2025;8:279. doi:10.1038/s42004-025-01665-1
10. Oh HSe-H, Urey DY, Karlsson L, et al. A cerebrospinal fluid synaptic protein biomarker for prediction of cognitive resilience versus decline in Alzheimer's disease. *Nat Med*. 2025;31:1592-1603. doi:10.1038/s41591-025-03565-2
11. Imam F, Saloner R, Vogel JW, et al. The Global neurodegeneration proteomics consortium: biomarker and drug target discovery for common neurodegenerative diseases and aging. *Nat Med*. 2025;31:2556-2566. doi:10.1038/s41591-025-03834-0
12. Afshar S, Dammer EB, Bian S, et al. Plasma proteomic associations with Alzheimer's disease endophenotypes. *Nat Aging*. 2025;5:2104-2124. doi:10.1038/s43587-025-00965-4
13. Wang Z, Chen Y, Gong K, et al. Cerebrospinal fluid proteomics identification of biomarkers for amyloid and tau PET stages. *Cell Reports Med*. 2025;6(4):102031. doi:10.1016/j.xcrm.2025.102031
14. Duggan MR, Gomez GT, Joynes CM, et al. Proteome-wide analysis identifies plasma immune regulators of amyloid-beta progression. *Brain Behav Immun*. 2024;120:604-619. doi:10.1016/j.bbi.2024.07.002
15. Mohs RC, Beauregard DW, Hughes L, et al. Biomarkers in patients with clinical signs of mild cognitive impairment or mild Alzheimer's disease but without amyloid deposits on positron emission tomography: results from Bio-Hermes study participants. *Alzheimer's Dement*. 2026;22:e71085. doi:10.1002/alz.71085
16. Morris JC, Weintraub S, Chui HC, et al. The Uniform Data Set (UDS): clinical and cognitive variables and descriptive data from Alzheimer disease centers. *Alzheimer Dis Assoc Disord*. 2006;20:210-216. doi:10.1097/01.wad.0000213865.09806.92
17. Mohs RC, Beauregard D, Dwyer J, et al. The Bio-Hermes Study: biomarker database developed to investigate blood-based and digital biomarkers in community-based, diverse populations clinically screened for Alzheimer's disease. *Alzheimers Dement*. 2024;20:2752-2765. doi:10.1002/alz.13722
18. Fagan AM, Roe CM, Xiong C, Mintun MA, Morris JC, Holtzman DM. Cerebrospinal fluid tau/beta-amyloid(42) ratio as a prediction of cognitive decline in nondemented older adults. *Arch Neurol*. 2007;64:343-349. doi:10.1001/archneur.64.3.noc60123
19. Ali M, Timsina J, Western D, et al. Multi-cohort cerebrospinal fluid proteomics identifies robust molecular signatures across the Alzheimer disease continuum. *Neuron*. 2025;113:1363-1379. doi:10.1016/j.neuron.2025.02.014
20. Duggan MR, Peng Z, Sipilä PN, et al. Proteomics identifies potential immunological drivers of postinfection brain atrophy and cognitive decline. *Nat Aging*. 2024;4:1263-1278. doi:10.1038/s43587-024-00682-4
21. Eldjarn GH, Ferkingstad E, Lund SH, et al. Large-scale plasma proteomics comparisons through genetics and disease associations. *Nature*. 2023;622:348-358. doi:10.1038/s41586-023-06563-x
22. Gold L, Ayers D, Bertino J, et al. Aptamer-based multiplexed proteomic technology for biomarker discovery. *PLoS One*. 2010;5:e15004. doi:10.1371/journal.pone.0015004
23. Timsina J, Gomez-Fonseca D, Wang L, et al. Comparative analysis of Alzheimer's Disease cerebrospinal fluid biomarkers measurement by Multiplex SOMAscan Platform and Immunoassay-Based approach. *J Alzheimers Dis*. 2022;89:193-207. doi:10.3233/JAD-220399
24. Yang C, Farias FHG, Ibanez L, et al. Genomic atlas of the proteome from brain, CSF and plasma prioritizes proteins implicated in neurological disorders. *Nat Neurosci*. 2021;24:1302-1312. doi:10.1038/s41593-021-00886-6
25. Ali M, Sung YJ, Wang F, Fernández M, Morris J, Fagan A, et al. Leveraging large multi-center cohorts of Alzheimer disease endophenotypes to understand the role of Klotho heterozygosity on disease risk 2021. doi:10.1101/2021.10.07.21264646 medRxiv
26. Timsina J, Ali M, Do A, et al. Harmonization of CSF and imaging biomarkers in Alzheimer's disease: need and practical applications for genetics studies and preclinical classification. *Neurobiol Dis*. 2024;190:106373. doi:10.1016/j.nbd.2023.106373
27. Deming Y, Li Z, Kapoor M, et al. Genome-wide association study identifies four novel loci associated with Alzheimer's endophenotypes

and disease modifiers. *Acta Neuropathol*. 2017;133(5):839-856. doi:10.1007/s00401-017-1685-y
28. Bartlett JW, Frost C, Mattsson N, et al. Determining cut-points for Alzheimer's disease biomarkers: statistical issues, methods and challenges. *Biomark Med*. 2012;6:391-400. doi:10.2217/bmm.12.49
29. Sojkova J, Goh J, Bilgel M, et al. Voxelwise Relationships between distribution volume ratio and cerebral blood flow: implications for analysis of β-Amyloid images. *J Nucl Med*. 2015;56:1042-1047. doi:10.2967/jnumed.114.151480
30. Kim H-Y. Statistical notes for clinical researchers: nonparametric statistical methods: 1. Nonparametric methods for comparing two groups. *Restor Dent Endod*. 2014;39:235-239. doi:10.5395/rde.2014.39.3.235
31. Wu T, Hu E, Xu S, et al. clusterProfiler 4.0: a universal enrichment tool for interpreting omics data. *Innov*. 2021;2:100141. doi:10.1016/j.xinn.2021.100141
32. Gillespie M, Jassal B, Stephan R, et al. The reactome pathway knowledgebase 2022. *Nucleic Acids Res*. 2022;50:D687-92. doi:10.1093/nar/gkab1028
33. The Gene Ontology Consortium. The Gene Ontology Resource: 20 years and still Going strong. *Nucleic Acids Res*. 2019. 47:D330–D338. doi:10.1093/nar/gky1055
34. Kanehisa M, KEGG: kyoto encyclopedia of genes and genomes. *Nucleic Acids Res*. 2000;28:27-30. doi:10.1093/nar/28.1.27
35. Agrawal A, Balcı H, Hanspers K, et al. WikiPathways 2024: next generation pathway database. *Nucleic Acids Res*. 2024;52:D679-89. doi:10.1093/nar/gkad960
36. Schriml LM, Munro JB, Schor M, et al. The Human Disease Ontology 2022 update. *Nucleic Acids Res*. 2022;50:D1255-61. doi:10.1093/nar/gkab1063
37. Tibshirani R, Walther G, Hastie T. Estimating the number of clusters in a data set via the gap statistic. *J R Stat Soc Ser B Stat Methodol*. 2001;63:411-423. doi:10.1111/1467-9868.00293
38. Lisboa PJG, Etchells TA, Jarman IH, Chambers SJ. Finding reproducible cluster partitions for the k-means algorithm. *BMC Bioinformatics*. 2013;14 Suppl 1(Suppl 1): S8. doi:10.1186/1471-2105-14-S1-S8
39. Woodbury ME, Ikezu T. Fibroblast growth factor-2 signaling in neurogenesis and neurodegeneration. *J Neuroimmune Pharmacol Off J Soc NeuroImmune Pharmacol*. 2014;9:92-101. doi:10.1007/s11481-013-9501-5
40. Ghimire A, Rehman SA, Subhani A, et al. Mechanism of microglia-mediated neuroinflammation, associated cognitive dysfunction, and therapeutic updates in Alzheimer's disease. *HLife*. 2025;3:64-81. doi:10.1016/j.hlife.2024.11.006
41. Sola-Sevilla N, Puerta E. SIRT2 as a potential new therapeutic target for Alzheimer's disease. *Neural Regen Res*. 2024;19:124-131. doi:10.4103/1673-5374.375315
42. Elyaman W, Stern LJ, Jiang N, et al. Exploring the role of T cells in Alzheimer's and other neurodegenerative diseases: emerging therapeutic insights from the T Cells in the Brain symposium. *Alzheimers Dement*. 2025;21:e14548. doi:10.1002/alz.14548
43. Perluigi M, Di Domenico F, Barone E, Butterfield DA. mTOR in Alzheimer disease and its earlier stages: links to oxidative damage in the progression of this dementing disorder. *Free Radic Biol Med*. 2021;169:382-396. doi:10.1016/j.freeradbiomed.2021.04.025
44. Yan X-Z, Lai L, Ao Q, Tian X-H, Zhang Y-H. Interleukin-17A in Alzheimer's disease: recent advances and controversies. *Curr Neuropharmacol*. 2022;20:372-383. doi:10.2174/1570159×19666210823110004
45. de Vries LE, Huitinga I, Kessels HW, Swaab DF, Verhaagen J. The concept of resilience to Alzheimer's disease: current definitions and cellular and molecular mechanisms. *Mol Neurodegener*. 2024;19(1):33. doi:10.1186/s13024-024-00719-7
46. Norden DM, Fenn AM, Dugan A, Godbout JP. TGFβ produced by IL-10 redirected astrocytes attenuates microglial activation. *Glia*. 2014;62:881-895. doi:10.1002/glia.22647
47. Wong GC-N, Chow KH-M. DNA damage response-associated cell cycle re-entry and neuronal senescence in brain aging and Alzheimer's disease. *J Alzheimers Dis*. 2023;94:S429-51. doi:10.3233/JAD-220203
48. Kotani K, Yamada T, Gugliucci A. Paired measurements of paraoxonase 1 and serum amyloid A as useful disease markers. *Biomed Res Int*. 2013;2013:481437. doi:10.1155/2013/481437
49. Jang S, Jang WY, Choi M, et al. Serum amyloid A1 is involved in amyloid plaque aggregation and memory decline in amyloid beta abundant condition. *Transgenic Res*. 2019;28:499-508. doi:10.1007/s11248-019-00166-x
50. He X, Huang Y, Li B, Gong C-X, Schuchman EH. Deregulation of sphingolipid metabolism in Alzheimer's disease. *Neurobiol Aging*. 2010;31:398-408. doi:10.1016/j.neurobiolaging.2008.05.010
51. Giovagnoni C, Ali M, Eijssen LMT, et al. Altered sphingolipid function in Alzheimer's disease; a gene regulatory network approach. *Neurobiol Aging*. 2021;102:178-187. doi:10.1016/j.neurobiolaging.2021.02.001
52. Atkin G, Paulson H. Ubiquitin pathways in neurodegenerative disease. *Front Mol Neurosci*. 2014;7:63. doi:10.3389/fnmol.2014.00063
53. Guedes JR, Santana I, Cunha C, et al. MicroRNA deregulation and chemotaxis and phagocytosis impairment in Alzheimer's disease. *Alzheimer's Dement* 2016;3:7-17. doi:10.1016/j.dadm.2015.11.004
54. Zheng C, Zhou X-W, Wang J-Z. The dual roles of cytokines in Alzheimer's disease: update on interleukins, TNF-α, TGF-β and IFN-γ. *Transl Neurodegener*. 2016;5:7. doi:10.1186/s40035-016-0054-4
55. Burkewitz K, Zhang Y, Mair WB. AMPK at the Nexus of energetics and aging. *Cell Metab*. 2014;20:10-25. doi:10.1016/j.cmet.2014.03.002
56. Pi T, Zhou X-W, Cai L, et al. PI3K/Akt signaling pathway is involved in the neurotrophic effect of senegenin. *Mol Med Rep*. 2016;13:1257-1262. doi:10.3892/mmr.2015.4652
57. Ashton NJ, Brum WS, Di Molfetta G, et al. Diagnostic Accuracy of a plasma phosphorylated Tau 217 Immunoassay for Alzheimer disease pathology. *JAMA Neurol*. 2024;81:255-263. doi:10.1001/jamaneurol.2023.5319
58. Jansen WJ, Janssen O, Tijms BM, et al. Prevalence Estimates of amyloid abnormality across the Alzheimer disease clinical spectrum. *JAMA Neurol*. 2022;79:228-243. doi:10.1001/jamaneurol.2021.5216
59. Chang S, Reim K, Pedersen M, Neher E, Brose N, Taschenberger H. Complexin stabilizes newly primed synaptic vesicles and prevents their premature fusion at the mouse calyx of held synapse. *J Neurosci Off J Soc Neurosci*. 2015;35:8272-8290. doi:10.1523/JNEUROSCI.4841-14.2015
60. Sato Y, Kawashima K, Fukui E, Matsumoto H, Yoshizawa F, Sato Y. Functional analysis reveals that Tinagl1 is required for normal muscle development in mice through the activation of ERK signaling. *Biochim Biophys Acta—Mol Cell Res*. 2022;1869:119294. doi:10.1016/j.bbamcr.2022.119294
61. Ahmad W, Ebert PR. Suppression of a core metabolic enzyme dihydrolipoamide dehydrogenase (dld) protects against amyloid beta toxicity in C. elegans model of Alzheimer's disease. *Genes Dis*. 2021;8:849-866. doi:10.1016/j.gendis.2020.08.004
62. Rudrabhatla P. Role of protein phosphatase 2A in Alzheimer's disease. *Curr Alzheimer Res*. 2011;8:623-632. doi:10.2174/156720511796717168
63. Carlyle BC, Kandigian SE, Kreuzer J, et al. Synaptic proteins associated with cognitive performance and neuropathology in older humans revealed by multiplexed fractionated proteomics. *Neurobiol Aging*. 2021;105:99-114. doi:10.1016/j.neurobiolaging.2021.04.012
64. Lackie RE, Maciejewski A, Ostapchenko VG, et al. The Hsp70/Hsp90 Chaperone Machinery in Neurodegenerative Diseases. *Front Neurosci*. 2017;11:254. doi:10.3389/fnins.2017.00254
65. Dorval V, Fraser PE. SUMO on the road to neurodegeneration. *Biochim Biophys Acta*. 2007;1773:694-706. doi:10.1016/j.bbamcr.2007.03.017

66. Jack Jr. CR, Andrews JS, Beach TG, et al. Revised criteria for diagnosis and staging of Alzheimer's disease: Alzheimer's association workgroup. *Alzheimer's Dement*. 2024;20:5143-5169. doi:10.1002/alz.13859
67. Palmqvist S, Janelidze S, Stomrud E, et al. Performance of Fully Automated Plasma Assays as Screening Tests for Alzheimer Disease-Related β-Amyloid Status. *JAMA Neurol*. 2019;76:1060-1069. doi:10.1001/jamaneurol.2019.1632
68. Mattsson-Carlgren N, Leuzy A, Janelidze S, et al. The implications of different approaches to define AT(N) in Alzheimer disease. *Neurology*. 2020;94:e2233-44. doi:10.1212/WNL.0000000000009485
69. Heneka MT, Carson MJ, Khoury JEl, et al. Neuroinflammation in Alzheimer's disease. *Lancet Neurol*. 2015;14:388-405. doi:10.1016/S1474-4422(15)70016-5
70. Cummings J, Zhou Y, Lee G, Zhong K, Fonseca J, Cheng F. Alzheimer's disease drug development pipeline: 2024. *Alzheimer's Dement Transl Res Clin Interv*. 2024;10:e12465. doi:10.1002/trc2.12465
71. Higginbotham L, Ping L, Dammer EB, et al. Integrated proteomics reveals brain-based cerebrospinal fluid biomarkers in asymptomatic and symptomatic Alzheimer's disease. *Sci Adv*. 2020;6:43. doi:10.1126/sciadv.aaz9360
72. Hilal ML, Rosina E, Pedini G, Restivo L, Bagni C. Dysregulation of the mTOR-FMRP pathway and synaptic plasticity in an environmental model of ASD. *Mol Psychiatry*. 2025;30:1937-1951. doi:10.1038/s41380-024-02805-0
73. Han P, Liang W, Baxter LC, et al. Pituitary adenylate cyclase-activating polypeptide is reduced in Alzheimer disease. *Neurology*. 2014;82:1724-1728. doi:10.1212/WNL.0000000000000417
74. Huynh T-PV, Davis AA, Ulrich JD, Holtzman DM. Apolipoprotein E and Alzheimer's disease: the influence of apolipoprotein E on amyloid-β and other amyloidogenic proteins. *J Lipid Res*. 2017;58:824-836. doi:10.1194/jlr.R075481
75. Mubeen S, Tom Kodamullil A, Hofmann-Apitius M, Domingo-Fernández D. On the influence of several factors on pathway enrichment analysis. *Brief Bioinform*. 2022;23:bbac143. doi:10.1093/bib/bbac143

SUPPORTING INFORMATION

Additional supporting information can be found online in the Supporting Information section at the end of this article.

How to cite this article: Chen Y, Duggan MR, Timsina J, et al. Blood-based proteomic signature of amyloidosis: identification of novel regulators of amyloid load. *Alzheimer's Dement*. 2026;22:e71611. https://doi.org/10.1002/alz.71611